

Unexpected Photo-driven Linker-to-Node Hole Transfer in a Zirconium-Based Metal–Organic Framework

Boris V. Kramar[§], Anna S. Bondarenko[§], Benjamin T. Diroll[‡], Xiaodan Wang[‡], Kirk S. Schanze[‡],

Lin X. Chen^{§,f}, Roel Tempelaar^{§*} and Joseph T. Hupp^{§*}*

[§]Department of Chemistry, Northwestern University, 2145 Sheridan Road, Evanston, Illinois 60208, United States

[‡]Nanoscience and Technology Division, Argonne National Laboratory, Argonne, Illinois 60439, United States

[Chemical Sciences and Engineering Division, Argonne National Laboratory, Argonne, Illinois 60439, United States

[‡]Department of Chemistry, University of Texas at San Antonio, One UTSA Circle, San Antonio, Texas 78249, United States

Authors:

Boris V. Kramar – Department of Chemistry, Northwestern University, 2145 Sheridan Road, Evanston, Illinois 60208, United States

Anna S. Bondarenko – Department of Chemistry, Northwestern University, 2145 Sheridan Road, Evanston, Illinois 60208, United States

Benjamin T. Diroll – Chemical Sciences and Engineering Division, Argonne National Laboratory, Argonne, Illinois 60439, United States

Xiaodan Wang – Department of Chemistry, University of Texas at San Antonio, One UTSA Circle, San Antonio, Texas 78249, United States

Kirk S. Schanze – Department of Chemistry, University of Texas at San Antonio, One UTSA Circle, San Antonio, Texas 78249, United States

Corresponding Authors:

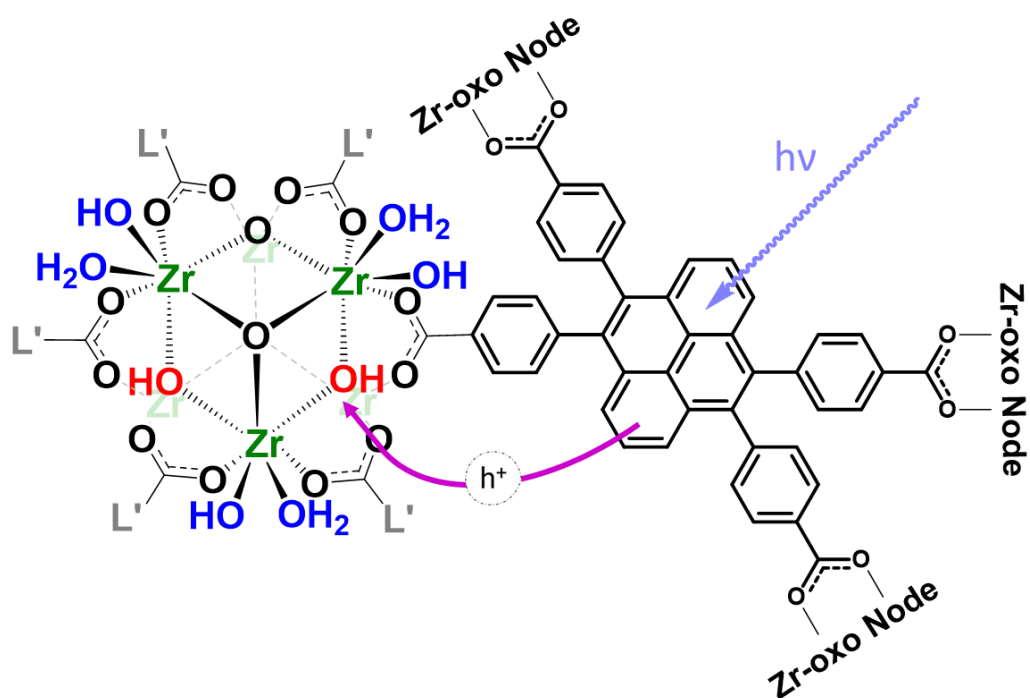
Joseph T. Hupp – Department of Chemistry, Northwestern University, 2145 Sheridan Road, Evanston, Illinois 60208, United States; <https://orcid.org/0000-0003-3982-9812>; Email: j-hupp@northwestern.edu

Lin X. Chen – Department of Chemistry, Northwestern University, 2145 Sheridan Road, Evanston, Illinois 60208, United States; <https://orcid.org/0000-0002-8450-6687>; Email: l-chen@northwestern.edu

Roel Tempelaar – Department of Chemistry, Northwestern University, 2145 Sheridan Road, Evanston, Illinois 60208, United States; <https://orcid.org/0000-0003-0786-7304>; Email: roel.tempelaar@northwestern.edu

ABSTRACT

$Zr_6(\mu_3-O)_4(\mu_3-OH)_4$ node cores are indispensable building blocks for almost all zirconium-based metal–organic frameworks. Consistent with the insulating nature of zirconia, they are generally considered electronically inert. Contrasting this viewpoint, we present spectral measurements and calculations indicating that emission from photoexcited NU-601, a six-connected Zr-based MOF, comes from both linker-centric locally-excited and linker-to-node charge-transfer (CT) states. The CT state originates from a hole transfer process enabled by favorable energy alignment of the HOMOs of the node and linker. This alignment can be manipulated by changing the pH of the medium, which alters the protonation state of multiple oxy groups on the Zr-node. Thus, the acid-base chemistry of the node has a direct effect on the photophysics of the MOF following linker-localized electronic excitation. These new findings open opportunities to understand and exploit, for energy conversion, unconventional mechanisms of exciton formation and transport in MOFs.



MAIN TEXT

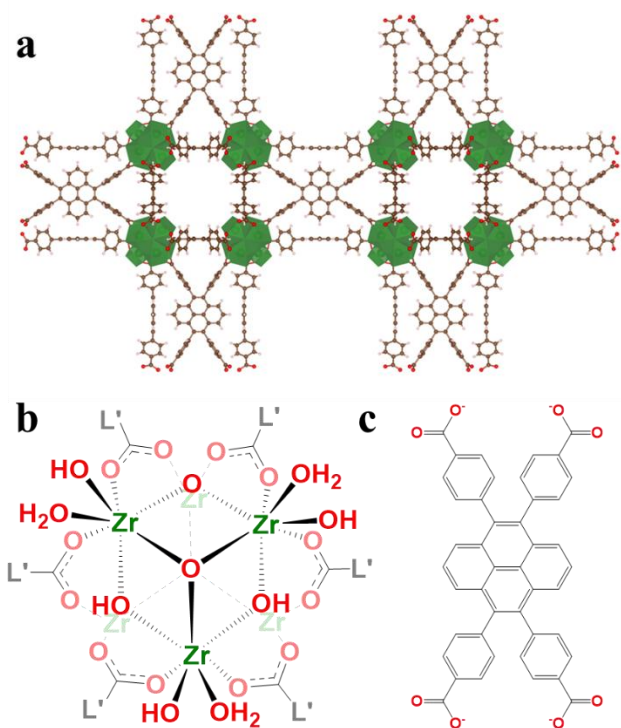
Zirconium-based metal–organic frameworks (Zr-MOFs) are promising light-harvesting platforms due to their high porosity, stability, and topological variety,¹⁻¹⁰ as well as their ability to organize chromophores (organic linkers) for extended, directional transport of photo-generated molecular excitons. In favorable instances, hundreds of linkers can be enlisted for propagation of a single exciton, collections of linkers can function as antennae, and, via terminal exciton splitting, frameworks can deliver oxidizing or reducing equivalents to sites far removed from the point of optical excitation.¹¹⁻¹⁴ Notably, if the sites are coupled to catalysts or electrodes, photonic energy can, in principle, be converted to stored chemical or useable electrical energy.

Importantly, a widely used node core for Zr-MOFs, $Zr_6(\mu_3-O)_4(\mu_3-OH)_4^{12+}$, is believed, based on the large and unfavorably positioned optical gap of ZrO_2 ,^{15, 16} to be optoelectronically inert. Having zero valence electrons, Zr(IV) cannot be chemically oxidized. Furthermore, apart from high-temperature reaction of zirconia with H_2 to form lattice oxygen vacancies and water vapor,¹⁷ chemical reduction of Zr(IV) in oxy ligand environments is almost never encountered.

The redox-inert nature of oxy-Zr(IV) species prevents unwanted redox-quenching of photo-generated excited-states, while also ensuring that frameworks are not disrupted by reduction-engendered weakening of metal (node)/oxy-anion (linker) bonds or restructuring of coordination motifs. Additionally, Truhlar *et al.* and others have shown computationally that photo-driven (visible or near-UV) linker-to-zirconium electron-transfer, is, in general, energetically unfavorable,^{16, 18, 19} and Patwardhan, *et al.* have shown that electronic-coupling-controlled, redox-hopping between linkers can be well understood by altogether neglecting Zr(IV).²⁰

Given the apparent redox-innocence of Zr(IV) and the seeming electronic energetic misalignment of linkers and nodes, we were surprised to find that fluorescence of the Zr-MOF, NU-601 (**Scheme 1**), following linker-localized photoexcitation, is strongly dependent on the extent of “inert” node

protonation. Indeed, both the fluorescence intensity and lineshape change drastically, but reversibly, with solution pH. Experiments and computations reveal intense, pH-tunable photo-emission from a rapidly formed, but indirectly populated linker-to-node charge-transfer (CT) state. The transferred charge, however, is a hole rather than an electron, and the charge acceptor is an oxygenic, rather than metal-ion, component of the node. While not developed here, the prevalence of this unusual excited-state could have profound mechanistic implications for energy transport and antenna behavior in photo-active Zr-MOFs.



Scheme 1. Structure of NU-601 (a);²¹ Zr node shown from c-axis: all six linker connections and half the core and nonstructural oxygenic ligands (b). L' represents the rest of the linker (c). Each linker connects to four nodes.

NU-601 is a six-connected MOF containing pyrene-derived linkers.²¹ The experimental absorption spectrum of the solubilized linker (**Fig. 1**) features a weak transition at ~ 3.27 eV (370 nm, highlighted), located below the principal transition at 3.55 eV. Time-dependent density-functional-theory (TD-DFT) calculations (**SI Section S3**) associate this weak transition with a transition dipole along the long axis of the pyrene. No Stokes shift is observed between the lowest energy

absorption band and the 0-0 fluorescence peak. We anticipated that NU-601 would display similar emission, since its nearest-neighbor linkers/chromophores: 1) are separated by Zr-nodes or by pores with center-to-center distances $>10 \text{ \AA}$, and 2) possess transition dipoles oriented 90° with respect to each other. Notably, these structural features should largely preclude both linker-to-linker resonance energy transfer and excimer formation.^{22, 4, 23} NU-901's emission maximum (in DMF) is $\sim 2.97 \text{ eV}$. At first glance, this seems to constitute a 0.30 eV bathochromic shift compared to the linker fluorescence spectrum. Closer inspection shows, however, that the 3.27 eV band is preserved in both the absorption and emission spectra of the MOF. The experimental absorption spectrum of the MOF is otherwise largely featureless, owing to the nature of diffuse-reflectance measurement; for this reason, absorption spectrum computation was not performed.

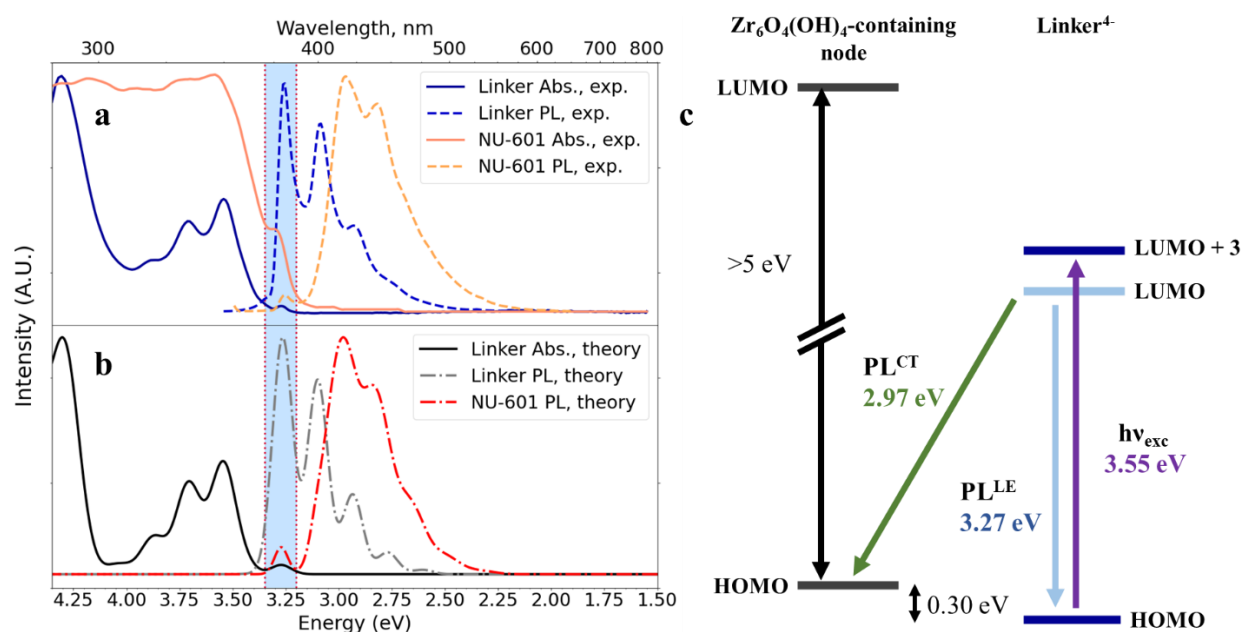


Figure 1. Experimental (a) and theoretical (b) absorption and emission spectra of NU-601 and its linker in dimethylformide (DMF). The energy diagram to the right (c) shows the relevant transitions. HOMO \rightarrow LUMO+3 is the dominant contributor to the principal transition at 3.55 eV . The HOMO-LUMO gap of the oxy-Zr node is assumed to exceed 5 eV .²⁴

We modeled all spectra based on a vibronic transition model, parametrized against *ab initio* calculations and experimental data (**SI Section S3**). TD-DFT calculations of the linker show that the principal transition at 3.55 eV is dominated by a HOMO to LUMO+3 transition. The transition

corresponding to the direct HOMO–LUMO gap possesses much less oscillator strength. Replication of the dominant MOF emission feature at 2.97 eV alongside the observable HOMO–LUMO linker absorption requires inclusion of an emitting state consistent with an indirectly formed linker-to-node CT state. Although not explored, previous computational work for the Zr-MOF UiO-66 (featuring a chemically-related linker) showed a proximal energy alignment between linker and node HOMOs, making linker*-to-node hole transfer (**Fig. 1c**) plausible.¹⁶ (Linker* denotes photo-excited linker.)

Based on our spectral analysis, we posit linker*-to-node hole transfer in NU-601 giving rise to a CT state emitting at 2.97 eV, with a 0.30 eV redshift relative to the HOMO-LUMO transition in the linker-centered excitation, henceforth referred to as locally-excited (LE) state (**Fig. 1c**). The conduction band-edge energy of ZrO₂ (used to approximate node LUMO) lies very high on an absolute energy scale, ruling out electron transfer from photo-excited linkers to Zr-nodes to yield Zr(III) (**SI Section S3**). Hole transfer, however, has seen little discussion (apart from through-space transfer to node-*appended* metal-ions or molecules).^{8, 11, 25, 26} We propose that the CT state forms as a state spectrally distinct from the LE state, but with both contributing to the total emission spectrum.²⁷ Moreover, the CT state evolves from the LE state and is facilitated by the periodic donor-acceptor like structure of the MOF, with excited linkers serving as hole donors and nodes as hole acceptors.^{28, 29}

To further substantiate the CT state assignment, we consider variations in the solvent environment. Changes in polarity and/or viscosity^{30,31} of the framework-permeating solvent engender only slight changes in the energy of the excited state (**SI Sections S5 & S6**). In contrast, varying the pH of the aqueous medium in the 1.5 to 8.5 range lead to a pronounced modulation of the emission lineshape and overall quantum yield, particularly that of the linker-based HOMO–LUMO emission band, consistent with populations of both CT and LE states being pH-dependent

(Fig. 2f, g). Similar, but subtler effects are observed in methanol (Fig. S7a). Clearly, the extent of CT state formation is connected to the protonation state of the node.

Transient fluorescence studies (SI Section S11) show that the overall emissive state lifetime varies from about 20 ns at near-neutral pH to about 5 ns in a highly acidic environment, and spectral evolution is consistent with what is observed in the steady state. It is tempting to ascribe lifetime attenuation in acid to participation of μ_3 -O-H stretches as high-frequency energy acceptors for nonradiative decay – an influence that ought to be present only if hole-transfer to hydroxobearing nodes occurs.^{32, 33}

To better understand pH influences, consider the $Zr_6O_4(OH)_4$ -containing node in a modulator- and formate-free Zr-MOF.³⁴ Below the maximum connectivity of 12,³⁵ sites that would otherwise be occupied by linker-terminating carboxylates instead feature nonstructural hydroxo and aqua ligands in equal numbers. The oxygen sites present are bridging oxo, bridging hydroxo, terminal hydroxo, terminal aqua, and carboxylate. Three of these five carry protons (Scheme 1b). Notably, pK_a values for the protonated sites, on Zr-MOF nodes, have previously been determined.³⁶⁻³⁸ The presence of multiple distinct pK_a values means that the node can be treated as a polyprotic acid. The Henderson-Hasselbalch equations can be used to obtain populations of various deprotonated node species as a function of pH (Fig. 2a-e).³⁹ We use 3.3, 5.7 and 8.2 as pK_a estimates for NU-601; these values are representative across a range of Zr-MOFs.³⁶⁻³⁸ In relating CT state formation to node protonation, we consider both average bulk populations and the probability of finding at least one of four linker-connected nodes in a given protonation state (Fig. 2a). Neglected is another pK_a , likely <1, corresponding to conditions where six terminal hydroxos have been converted to six additional $-OH_2$ ligands.³⁴

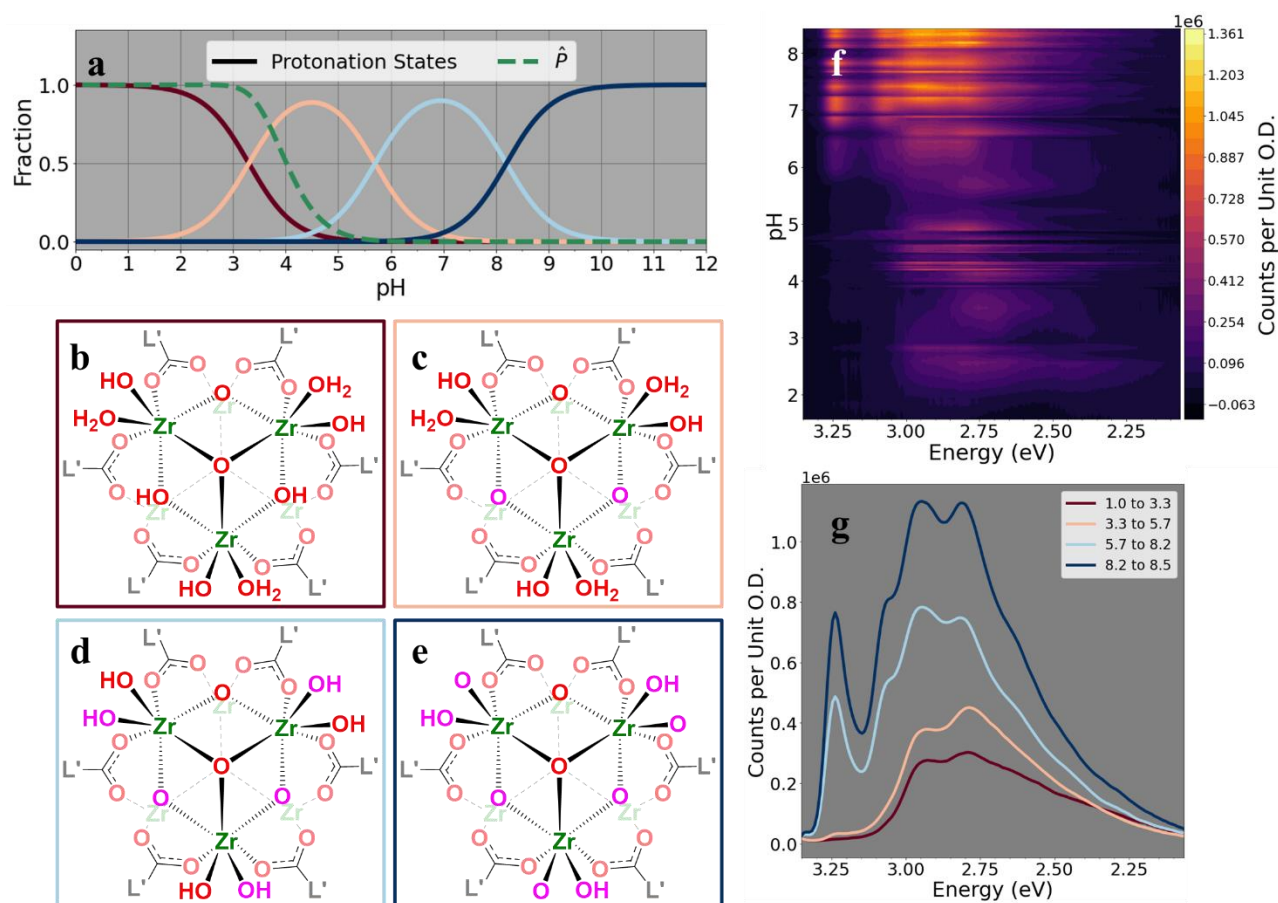


Figure 2. a) Distribution of various node protonation states as a function of pH, based on the pK_a values reported by Klet et al.³⁶ \hat{P} represents the probability of having at least one of four tetratopic-linker-connected nodes with a bridging-hydroxo proton still in place; see **SI Section S2**. b) – e) Schematic depictions of the Zr node, shown with all six linkers and half of the node's oxygenic groups. Schemes are arranged to show successive deprotonation. Emission as a function of pH is pooled in the contour plot (f) and binned along the pH axis into bins defined by pK_a values (g). Curves in a) and g) and outlines in b) – e) are color-coded.

We suggest two main effects that drive the pH dependence of the excited-state properties: (1) the Coulombic interactions that should promote linker*-to-node hole transfer based on charge changes upon node deprotonation (**Fig. 3a**); and (2) the rise of the HOMO energy level of the node with deprotonation shown by our TD-DFT calculations, implying that deprotonation of the node breaks the linker-node orbital energy alignment and shifts the LE/CT excited-state distribution (**Fig. 3b**). In fact, our calculations show a large increase in the HOMO-HOMO energy gap — albeit, with only an approximate estimate since the calculated cluster comprises one node with six benzoate “caps” instead of full linkers (**Fig. 3c** and **SI Section S3**). Linear combination

fitting (LCF) (**Fig. 3d-g**) of pH-binned spectra to theoretical LE and CT fluorescence lineshapes captures the appearance of the LE contribution, but also clearly shows that the CT contribution is dominant regardless of pH, in contrast to the populations predicted by acid equilibrium (**Fig. 2a**). This implies that multiple physical effects are relevant and that neither of the arguments can be taken in isolation. At the simplest level, linker*-to-node CT state formation is pairwise; thus, we suggest that the persistence of the CT state across the entire pH range may be explained by the fact that a linker can always find a node to which it can transfer a hole. The probability of a linker being connected to at least one node with a μ_3 -OH protons still in place falls to 1% at about pH 6.4 (**Fig. 2a**); both linker-to-linker exciton hopping and dynamic protonation presumably would increase the likelihood of an encounter between an LE-type exciton and a protonated node, and extend the pH range.⁴⁰ Additionally, the 33% share of the LE contribution observed at high pH appears to be consistent with the 1:1.5 node-linker stoichiometry in NU-601; assuming similar quantum yields, we can hypothesize that at high pH CT state population is saturated.

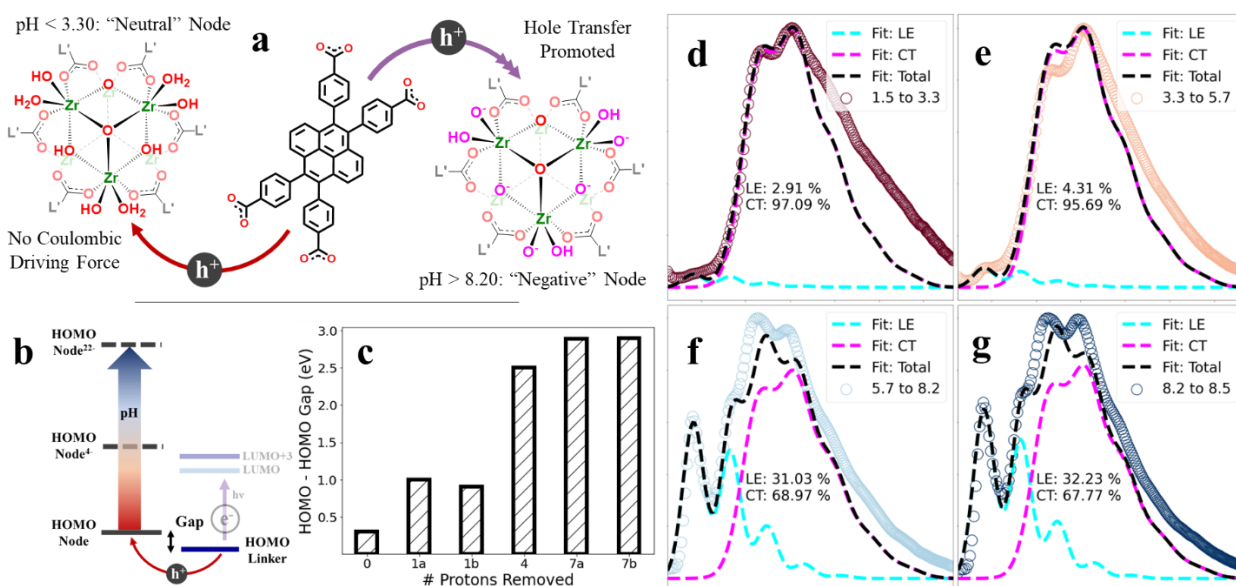


Figure 3. Schematic representation of the Coulombic argument in linker*-to-node hole transfer (a), the effect of deprotonation on the node HOMO level (b) and the resulting computed HOMO-HOMO gap (c), and linear combination fitting of compound pH-dependent fluorescence spectrum to the computed LE and CT state contributions (d-g).

Since LCF was insufficient to reconstruct emission signatures as a function of pH, we turned to principal component analysis (PCA). This method decomposes the observed data into multiple best-fit contributors. The optimal number of contributors can be determined via singular value decomposition (**SI Section S10**). Ratios of contributions vary with pH. Consequently, the Henderson-Hasselbalch equations can be used as a mechanistic model to guide PCA. Within the routine, pK_a values are allowed to vary; since fluorescence reports on excited states, the best fit pK_a values here must correspond to excited-state pK_a values, pK_a^* (for additional discussion, see **SI Section S2**). In the specific case of hole transfer to the node, we expect at least one pK_a^* value to decrease compared to ground-state pK_a due to net increase in positive charge on the node. PCA results are shown in **Fig. 4b** and **4c**. We fit data to three components (two pK_a^* values), because this is sufficient to describe the data (see **Fig. S10**). The analysis returns pK_a^* values of 2.0 and 6.6 with negligible fitting uncertainties.

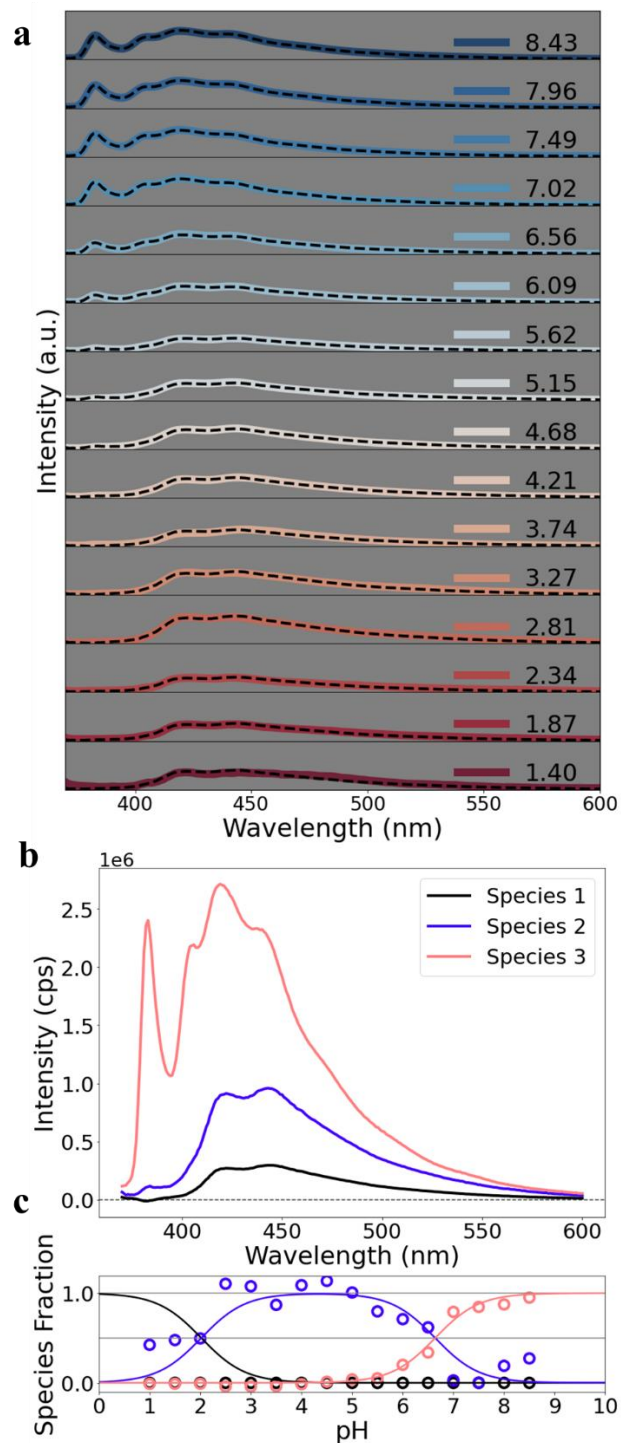
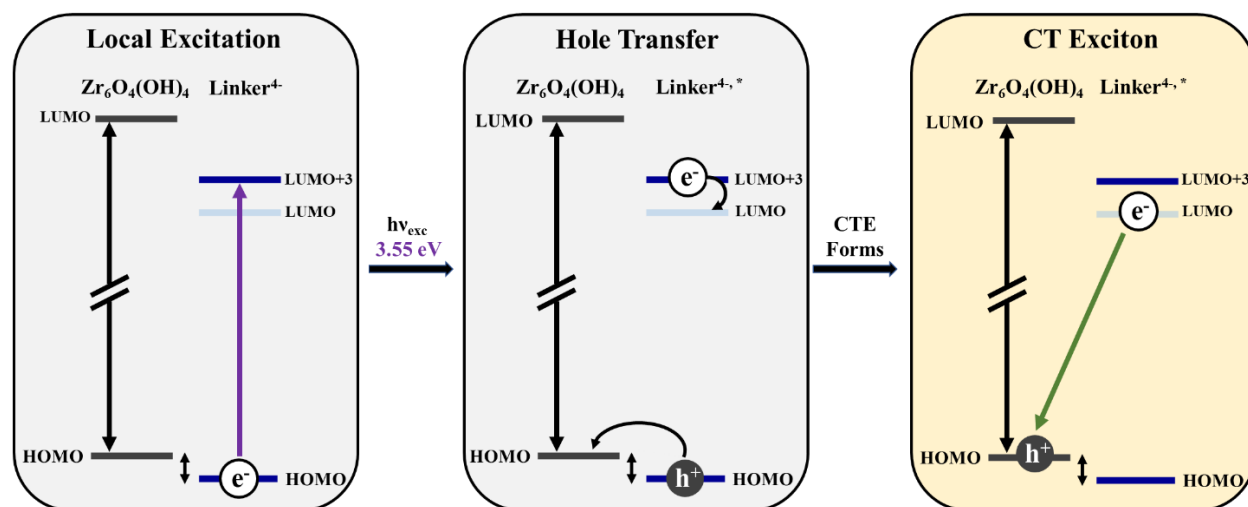


Figure 4. Fluorescence spectra (a) from **Fig. 2f** rebinned with respect to pH, plotted with fits described by b) species-associated spectra extracted via global fitting to Henderson-Hasselbalch equations, and c) the corresponding species-associated populations versus pH.

Typically, K_a^* for a photoacid will be higher than that for the ground state K_a by several orders of magnitude,^{41, 42} although smaller changes – i.e., $\Delta pK_a \approx 1$ – aren't uncommon.⁴³ While three pK_a s have been measured for the node in the ground state, only two are necessary to describe the excited state. We infer that the pK_a^* of 2.0 corresponds to the ground state pK_a of 3.3, reflecting the increased acidity of μ_3 -hydroxos upon hole injection. There is a concurrent decrease in acidity of aqua ligands from GS $pK_a=5.8$ to $pK_a^*=6.6$.

Experimental emission spectra and accompanying theory work evince communication between LE and CT states, where the charge-transfer state is formed by linker*-to-node hole transfer (**Scheme 2**). This notion is substantiated by node protonation influencing emission despite the node not being part of the absorbing chromophore. However, the high-pH spectral contributor (**Fig. 4b, Species 3**) extracted through target analysis does not perfectly match the theoretical LE lineshape from **Fig. 3d-g**, suggesting that the high-pH component is a mix of LE and CT states. This picture is consistent with the presented explanation of electronic effects (node HOMO level affected by pH) in competition with Coulombic effects (diminished positive charge on the node core promoting hole transfer). The presence of solvent electrolyte was also found to have an effect; the CT state may be stabilized at a higher pH by compensating the missing protons with alkali metal cations (see **Fig. S8**).



Scheme 2: Summary of the CT exciton formation mechanism.

The presence of the CT state has important implications for Zr-MOFs in photochemical applications, especially those involving/requiring antenna behavior and long-range energy transport. As an alternative to FRET (Förster resonance energy transfer),⁴⁴ the state may offer a basis for energy transport via an unconventional superexchange mechanism, first described by Haarer, et al., where LE states facilitate charge-carrier tunneling.^{28, 45} Broadly, this would mean that the optoelectronic properties of selected Zr-MOFs are dependent on formation of CT states or excitons, as opposed to the LE-dominated behavior observed in MOFs such as NH₂-MIL-53 and ZIF-67.^{46, 47} We speculate that the reported fluorescence sensitivity of NU-1000 to cyanide-containing solutions is a manifestation of tuning of an emissive linker*-to-node CT state, like that explored here for NU-901. We further suggest that the unusually large fluorescence Stokes shift for NU-1000 reflects emission from a different state (linker*-to-node hole-transfer) than the one created by absorption (linker-localized excitation). Closely related may be the ability of NU-1000 to propagate photo-generated excitons across hundreds of linkers, despite minimal overlap of absorption and fluorescence spectra. If energy transport is accomplished by the abovementioned, CT-enabled Haarer-superexchange mechanism, rather than FRET, such overlap wouldn't be needed. Assessment of the potential quantitative applicability of the CT-enabled scheme to long-range energy transport within selected Zr-MOFs is a focus of ongoing work.

EXPERIMENTAL METHODS

The experimental methods are described in the Supporting Information.

ASSOCIATED CONTENT

Supporting Information: Experimental methods (synthesis, data collection, data treatment, theory); nuclear magnetic resonance (NMR) spectra; powder X-ray diffraction (PXRD) data; N₂ sorption data; additional sets of emission data in different solvent environments; SEM images; FLIM images; experiments with methyl viologen; time-resolved emission; and additional discussion.

AUTHOR INFORMATION

Authors:

Boris V. Kramar – Department of Chemistry, Northwestern University, 2145 Sheridan Road, Evanston, Illinois 60208, United States; <https://orcid.org/0000-0001-8731-7542>; Email: boriskramar2023@u.northwestern.edu

Anna S. Bondarenko – Department of Chemistry, Northwestern University, 2145 Sheridan Road, Evanston, Illinois 60208, United States; Email: anna.bondarenko@northwestern.edu

Benjamin T. Diroll – Chemical Sciences and Engineering Division, Argonne National Laboratory, Argonne, Illinois 60439, United States; <https://orcid.org/0000-0003-3488-0213>; Email: bdiroll@anl.gov

Xiaodan Wang – Department of Chemistry, University of Texas at San Antonio, One UTSA Circle, San Antonio, Texas 78249, United States; Email: xiaodan.wang@utsa.edu

Kirk S. Schanze – Department of Chemistry, University of Texas at San Antonio, One UTSA Circle, San Antonio, Texas 78249, United States; <https://orcid.org/0000-0003-3342-4080>; Email: kirk.schanze@utsa.edu

Corresponding Authors:

Joseph T. Hupp – Department of Chemistry, Northwestern University, 2145 Sheridan Road, Evanston, Illinois 60208, United States; <https://orcid.org/0000-0003-3982-9812>; Email: j-hupp@northwestern.edu

Lin X. Chen – Department of Chemistry, Northwestern University, 2145 Sheridan Road, Evanston, Illinois 60208, United States; <https://orcid.org/0000-0002-8450-6687>; Email: l-x.chen@northwestern.edu

Roel Tempelaar – Department of Chemistry, Northwestern University, 2145 Sheridan Road, Evanston, Illinois 60208, United States; <https://orcid.org/0000-0003-0786-7304>; Email: roel.tempelaar@northwestern.edu

NOTES

The authors declare no competing financial interests.

ACKNOWLEDGMENTS

J.T.H. gratefully acknowledges support from the U.S. Dept. of Energy, Office of Science, Basic Energy Sciences, Solar Photochemistry Program (grant numbers DE-FG02-87ER-13808). Work performed at the Center for Nanoscale Materials, a U.S. Department of Energy Office of Science User Facility, was supported by the U.S. DOE, Office of Basic Energy Sciences, under Contract No. DE-AC02-06CH11357. A.S.B. and R.T. acknowledge support from the National Science Foundation under Grant No. CHE-2145433. B.V.K. is partially supported by a MURI Grant from ONR (N00014-20-1-2517) to L.X.C. The effort of L.X.C. is partially supported by the U.S.

Department of Energy, Office of Science, Office of Basic Energy Sciences, under Contract No. DE-AC02-06CH11357.

References

- (1) Wang, J.-L.; Wang, C.; Lin, W. Metal–Organic Frameworks for Light Harvesting and Photocatalysis. *ACS Catalysis* **2012**, *2* (12), 2630-2640. DOI: 10.1021/cs3005874.
- (2) Benseghir, Y.; Solé-Daura, A.; Cairnie, D. R.; Robinson, A. L.; Duguet, M.; Mialane, P.; Gairola, P.; Gomez-Mingot, M.; Fontecave, M.; Iovan, D.; et al. Unveiling the mechanism of the photocatalytic reduction of CO₂ to formate promoted by porphyrinic Zr-based metal–organic frameworks. *Journal of Materials Chemistry A* **2022**, *10* (35), 18103-18115, 10.1039/D2TA04164B. DOI: 10.1039/D2TA04164B.
- (3) Shaikh, S. M.; Chakraborty, A.; Alatis, J.; Cai, M.; Danilov, E.; Morris, A. J. Light harvesting and energy transfer in a porphyrin-based metal organic framework. *Faraday Discussions* **2019**, *216*, 174-190. DOI: 10.1039/c8fd00194d.
- (4) Shaikh, S. M.; Ilic, S.; Gibbons, B. J.; Yang, X.; Jakubikova, E.; Morris, A. J. Role of a 3D Structure in Energy Transfer in Mixed-Ligand Metal–Organic Frameworks. *The Journal of Physical Chemistry C* **2021**, *125* (42), 22998-23010. DOI: 10.1021/acs.jpcc.1c06427.
- (5) Shaikh, S. M.; Usov, P. M.; Zhu, J.; Cai, M.; Alatis, J.; Morris, A. J. Synthesis and Defect Characterization of Phase-Pure Zr-MOFs Based on Meso-tetracarboxyphenylporphyrin. *Inorganic Chemistry* **2019**, *58* (8), 5145-5153. DOI: 10.1021/acs.inorgchem.9b00200.
- (6) Deria, P.; Yu, J.; Balaraman, R. P.; Mashni, J.; White, S. N. Topology-dependent emissive properties of zirconium-based porphyrin MOFs. *Chemical Communications* **2016**, *52* (88), 13031-13034.
- (7) Deria, P.; Yu, J.; Smith, T.; Balaraman, R. P. Ground-State versus Excited-State Interchromophoric Interaction: Topology Dependent Excimer Contribution in Metal-Organic Framework Photophysics. *Journal of the American Chemical Society* **2017**, *139* (16), 5973-5983. DOI: 10.1021/jacs.7b02188.
- (8) Li, X.; Yu, J.; Gosztola, D. J.; Fry, H. C.; Deria, P. Wavelength-Dependent Energy and Charge Transfer in MOF: A Step toward Artificial Porous Light-Harvesting System. *Journal of the American Chemical Society* **2019**, *141* (42), 16849-16857. DOI: 10.1021/jacs.9b08078.
- (9) Rajasree, S. S.; Yu, J.; Pratik, S. M.; Li, X.; Wang, R.; Kumbhar, A. S.; Goswami, S.; Cramer, C. J.; Deria, P. Superradiance and Directional Exciton Migration in Metal–Organic Frameworks. *Journal of the American Chemical Society* **2022**, *144* (3), 1396-1406. DOI: 10.1021/jacs.1c11979.
- (10) Yu, J.; Li, X.; Deria, P. Light-Harvesting in Porous Crystalline Compositions: Where We Stand toward Robust Metal–Organic Frameworks. *ACS Sustainable Chemistry & Engineering* **2019**, *7* (2), 1841-1854. DOI: 10.1021/acssuschemeng.8b05673.
- (11) Goswami, S.; Yu, J.; Patwardhan, S.; Deria, P.; Hupp, J. T. Light-Harvesting “Antenna” Behavior in NU-1000. *ACS Energy Letters* **2021**, *6* (3), 848-853.
- (12) Kumagai, K.; Uematsu, T.; Torimoto, T.; Kuwabata, S. Photoluminescence Enhancement by Light Harvesting of Metal–Organic Frameworks Surrounding Semiconductor Quantum Dots. *Chemistry of Materials* **2021**, *33* (5), 1607-1617. DOI: 10.1021/acs.chemmater.0c03367.
- (13) Van Wyk, A.; Smith, T.; Park, J.; Deria, P. Charge-Transfer within Zr-Based Metal-Organic Framework: The Role of Polar Node. *Journal of the American Chemical Society* **2018**, *140* (8), 2756-2760. DOI: 10.1021/jacs.7b13211.
- (14) Liu, L.; Lu, X.-Y.; Zhang, M.-L.; Ren, Y.-X.; Wang, J.-J.; Yang, X.-G. 2D MOF nanosheets as an artificial light-harvesting system with enhanced photoelectric switching performance. *Inorganic Chemistry Frontiers* **2022**, *9* (11), 2676-2682, 10.1039/D2QI00404F. DOI: 10.1039/D2QI00404F.

- (15) Gionco, C.; Paganini, M. C.; Giamello, E.; Burgess, R.; Di Valentin, C.; Pacchioni, G. Cerium-Doped Zirconium Dioxide, a Visible-Light-Sensitive Photoactive Material of Third Generation. *The Journal of Physical Chemistry Letters* **2014**, *5* (3), 447-451. DOI: 10.1021/jz402731s.
- (16) Wu, X.-P.; Gagliardi, L.; Truhlar, D. G. Cerium Metal–Organic Framework for Photocatalysis. *Journal of the American Chemical Society* **2018**, *140* (25), 7904-7912. DOI: 10.1021/jacs.8b03613.
- (17) Eder, D.; Kramer, R. The stoichiometry of hydrogen reduced zirconia and its influence on catalytic activity Part 1: Volumetric and conductivity studies. *Physical Chemistry Chemical Physics* **2002**, *4* (5), 795-801, 10.1039/B109887J. DOI: 10.1039/B109887J.
- (18) Nasalevich, M. A.; Hendon, C. H.; Santaclara, J. G.; Svane, K.; van der Linden, B.; Veber, S. L.; Fedin, M. V.; Houtepen, A. J.; van der Veen, M. A.; Kapteijn, F.; et al. Electronic origins of photocatalytic activity in d0 metal organic frameworks. *Scientific Reports* **2016**, *6* (1), 23676-23676. DOI: 10.1038/srep23676.
- (19) Hendrickx, K.; Vanpoucke, D. E. P.; Leus, K.; Lejaeghere, K.; Van Yperen-De Deyne, A.; Van Speybroeck, V.; Van Der Voort, P.; Hemelsoet, K. Understanding Intrinsic Light Absorption Properties of UiO-66 Frameworks: A Combined Theoretical and Experimental Study. *Inorganic Chemistry* **2015**, *54* (22), 10701-10710. DOI: 10.1021/acs.inorgchem.5b01593.
- (20) Patwardhan, S.; Schatz, G. C. Theoretical Investigation of Charge Transfer in Metal Organic Frameworks for Electrochemical Device Applications. *The Journal of Physical Chemistry C* **2015**, *119* (43), 24238-24247. DOI: 10.1021/acs.jpcc.5b06065.
- (21) Lu, Z.; Wang, R.; Liao, Y.; Farha, O. K.; Bi, W.; Sheridan, T. R.; Zhang, K.; Duan, J.; Liu, J.; Hupp, J. T. Isomer of linker for NU-1000 yields a new she-type, catalytic, and hierarchically porous, Zr-based metal–organic framework. *Chemical Communications* **2021**, *57* (29), 3571-3574, 10.1039/D0CC07974J. DOI: 10.1039/D0CC07974J.
- (22) Wan, R.; Ha, D.-G.; Dou, J.-H.; Lee, W. S.; Chen, T.; Oppenheim, J. J.; Li, J.; Tisdale, W. A.; Dincă, M. Dipole-mediated exciton management strategy enabled by reticular chemistry. *Chemical Science* **2022**, *13* (36), 10792-10797, 10.1039/D2SC01127A. DOI: 10.1039/D2SC01127A.
- (23) Birks, J. B. Excimers. *Reports on Progress in Physics* **1975**, *38* (8), 903. DOI: 10.1088/0034-4885/38/8/001.
- (24) Emeline, A.; Kataeva, G. V.; Litke, A. S.; Rudakova, A. V.; Ryabchuk, V. K.; Serpone, N. Spectroscopic and Photoluminescence Studies of a Wide Band Gap Insulating Material: Powdered and Colloidal ZrO₂ Sols. *Langmuir* **1998**, *14* (18), 5011-5022. DOI: 10.1021/la980083l.
- (25) Kramar, B. V.; Flanders, N. C.; Helweh, W.; Dichtel, W. R.; Hupp, J. T.; Chen, L. X. Light Harvesting Antenna Properties of Framework Solids. *Accounts of Materials Research* **2022**, *3* (11), 1149-1159. DOI: 10.1021/accountsmr.2c00137.
- (26) Li, Q.; Li, D.; Wu, Z.-Q.; Shi, K.; Liu, T.-H.; Yin, H.-Y.; Cai, X.-B.; Fan, Z.-L.; Zhu, W.; Xue, D.-X. RhB-Embedded Zirconium–Biquinoline-Based MOF Composite for Highly Sensitive Probing Cr(VI) and Photochemical Removal of CrO₄²⁻, Cr₂O₇²⁻, and MO. *Inorganic Chemistry* **2022**, *61* (38), 15213-15224. DOI: 10.1021/acs.inorgchem.2c02459.
- (27) Qian, G.; Dai, B.; Luo, M.; Yu, D.; Zhan, J.; Zhang, Z.; Ma, D.; Wang, Z. Y. Band Gap Tunable, Donor–Acceptor–Donor Charge-Transfer Heteroquinoid-Based Chromophores: Near Infrared Photoluminescence and Electroluminescence. *Chemistry of Materials* **2008**, *20* (19), 6208-6216. DOI: 10.1021/cm801911n.
- (28) Haarer, D.; Philpott, M. R.; Morawitz, H. Field induced charge-transfer exciton transitions. *The Journal of Chemical Physics* **1975**, *63* (12), 5238-5245. DOI: 10.1063/1.431310 (accessed 2023/01/04).
- (29) Agranovich, V. M. *Excitations in Organic Solids*; Oxford University Press, 2008.
- (30) Sasaki, S.; Drummen, G. P. C.; Konishi, G.-i. Recent advances in twisted intramolecular charge transfer (TICT) fluorescence and related phenomena in materials chemistry. *Journal of Materials Chemistry C* **2016**, *4* (14), 2731-2743, 10.1039/C5TC03933A. DOI: 10.1039/C5TC03933A.

- (31) Yu, J.; Park, J.; Van Wyk, A.; Rumbles, G.; Deria, P. Excited-State Electronic Properties in Zr-Based Metal–Organic Frameworks as a Function of a Topological Network. *Journal of the American Chemical Society* **2018**, *140* (33), 10488-10496. DOI: 10.1021/jacs.8b04980.
- (32) Palit, D. K.; Pal, H.; Mukherjee, T.; Mittal, J. P. Photodynamics of the S1 state of some hydroxy- and amino-substituted naphthoquinones and anthraquinones. *Journal of the Chemical Society, Faraday Transactions* **1990**, *86* (23), 3861-3869, 10.1039/FT9908603861. DOI: 10.1039/FT9908603861.
- (33) Avouris, P.; Gelbart, W. M.; El-Sayed, M. A. Nonradiative electronic relaxation under collision-free conditions. *Chemical Reviews* **1977**, *77* (6), 793-833.
- (34) Lu, Z.; Liu, J.; Zhang, X.; Liao, Y.; Wang, R.; Zhang, K.; Lyu, J.; Farha, O. K.; Hupp, J. T. Node-Accessible Zirconium MOFs. *Journal of the American Chemical Society* **2020**, *142* (50), 21110-21121. DOI: 10.1021/jacs.0c09782.
- (35) Kaur, G.; Øien-Ødegaard, S.; Lazzarini, A.; Chavan, S. M.; Bordiga, S.; Lillerud, K. P.; Olsbye, U. Controlling the Synthesis of Metal–Organic Framework UiO-67 by Tuning Its Kinetic Driving Force. *Crystal Growth & Design* **2019**, *19* (8), 4246-4251. DOI: 10.1021/acs.cgd.9b00916.
- (36) Klet, R. C.; Liu, Y.; Wang, T. C.; Hupp, J. T.; Farha, O. K. Evaluation of Brønsted acidity and proton topology in Zr- and Hf-based metal–organic frameworks using potentiometric acid–base titration. *Journal of Materials Chemistry A* **2016**, *4* (4), 1479-1485, 10.1039/C5TA07687K. DOI: 10.1039/C5TA07687K.
- (37) Liao, Y. Investigation of Metal–Organic Frameworks in Chemical Separations and Catalysis. Ph.D., Northwestern University, United States -- Illinois, 2020.
- (38) Chen, H. Computational study of Brønsted acidity in the metal–organic framework UiO-66. *Chemical Physics Letters* **2022**, *800*, 139658. DOI: <https://doi.org/10.1016/j.cplett.2022.139658>.
- (39) Po, H. N.; Senozan, N. M. The Henderson-Hasselbalch Equation: Its History and Limitations. *Journal of Chemical Education* **2001**, *78* (11), 1499. DOI: 10.1021/ed078p1499.
- (40) Halder, A.; Bain, D. C.; Oktawiec, J.; Addicoat, M. A.; Tsangari, S.; Fuentes-Rivera, J. J.; Pitt, T. A.; Musser, A. J.; Milner, P. J. Enhancing Dynamic Spectral Diffusion in Metal–Organic Frameworks through Defect Engineering. *Journal of the American Chemical Society* **2023**, *145* (2), 1072-1082.
- (41) Solntsev, K. M.; Huppert, D.; Tolbert, L. M.; Agmon, N. Solvatochromic shifts of "super" photoacids. *Journal of the American Chemical Society* **1998**, *120* (31), 7981-7982.
- (42) Spies, C.; Shomer, S.; Finkler, B.; Pines, D.; Pines, E.; Jung, G.; Huppert, D. Solvent dependence of excited-state proton transfer from pyranine-derived photoacids. *Physical Chemistry Chemical Physics* **2014**, *16* (19), 9104-9114, 10.1039/C3CP55292F. DOI: 10.1039/C3CP55292F.
- (43) Chakraborty, S.; Nandi, S.; Bhattacharyya, K.; Mukherjee, S. Time Evolution of Local pH Around a Photo-Acid in Water and a Polymer Hydrogel: Time Resolved Fluorescence Spectroscopy of Pyranine. *ChemPhysChem* **2019**, *20* (23), 3221-3227, <https://doi.org/10.1002/cphc.201900845>. DOI: <https://doi.org/10.1002/cphc.201900845> (accessed 2022/11/01).
- (44) Förster, T. Energiewanderung und fluoreszenz. *Naturwissenschaften* **1946**, *33* (6), 166-175.
- (45) Schlesinger, I.; Powers-Riggs, N. E.; Logsdon, J. L.; Qi, Y.; Miller, S. A.; Tempelaar, R.; Young, R. M.; Wasielewski, M. R. Charge-transfer biexciton annihilation in a donor–acceptor co-crystal yields high-energy long-lived charge carriers. *Chemical Science* **2020**, *11* (35), 9532-9541, 10.1039/D0SC03301D. DOI: 10.1039/D0SC03301D.
- (46) Hanna, L.; Kucheryavy, P.; Liu, C.; Zhang, X.; Lockard, J. V. Long-Lived Photoinduced Charge Separation in a Trinuclear Iron- μ_3 -oxo-based Metal–Organic Framework. *Journal of Physical Chemistry C* **2017**, *121* (25), 13570-13576. DOI: 10.1021/acs.jpcc.7b03936.
- (47) Hu, W.; Yang, F.; Pietraszak, N.; Gu, J.; Huang, J. Distance Dependent Energy Transfer Dynamics from Molecular Donor to Zeolitic Imidazolate Framework Acceptor. *Physical Chemistry Chemical Physics* **2020**. DOI: 10.1039/D0CP03995K.